

Studies on Methanol, Ethanol, and Biomethanol Flame Structure

Akimasa Tsutsumi¹, Makihito Nishioka², and Keiichi Hori³

¹The Graduate University for Advanced Studies

Sagamihara, Kanagawa, Japan

² Department of Engineering Mechanics and Energy, University of Tsukuba

Tsukuba, Ibaraki, Japan

³ Institute of Space and Astronautical Science, Japan Aerospace Exploration Agency

Sagamihara, Kanagawa, Japan

1 Introduction

Much attention has been drawn recently to bio-fuel as alternative fuel. Bioethanol and biomethanol are well noted alternative fuel. Biomethanol is able to be produced from scrap wood or shredded paper; therefore, it is more suitable to use biomethanol than to use bioethanol. There are examples of research on combustion characteristics of methanol, however many of them are results which were conducted at idealized reaction field [1, 2] or for an internal-combustion engine [3]. The structure of counter flow methanol flame has been simulated by using a detail kinetic mechanism, and validated with experimental results [4]. However, the structure of two-dimensional methanol flame has not been researched well. A new vapor system for liquid bio-alcohol and a coflow burner were developed. Pure-ethanol was chosen to confirm stable combustion and to establish procedure of experiments. Flame temperature, concentrations of five stable chemical species, and fluorescence intensity of hydroxyl (OH) radical were measured respectively. The structure of two-dimensional ethanol flame was simulated by using a detailed chemical kinetic mechanism and compared to experimental results. Concerning methanol and biomethanol, flame temperature was measured.

2 Experimental and Numerical Procedure

2.1 Experimental Apparatus

Experiments were conducted in a laminar coflow configuration. A burner, a fuel feed system, and an ambient-airflow system are shown in Figure 1. Liquid ethanol (or methanol) was injected continuously by an infusion pump (CHEMIX “Fusion 200”). A mixer and all pipes were heated by ribbon heaters (SAKAGUCHI ELECTRIC HEATER). Alcohol fuel was vaporized by preheated nitrogen. The fuel vapor and nitrogen were mixed in the mixer which was an inner diameter of 46mm, an outer diameter of 50mm, and a long of 300mm. It had observation windows at both ends. Then, the mixed fuel gas flowed to an injection pipe which was heated by a heat tape (Clayborn Precision Heat Tape, “E-16”). The pipe was an outer diameter of 8mm, an inner diameter of 7mm, and a long of 1 meter.

Temperature of the fuel gas was measured by K-type sheathed thermocouples. Ambient air was straightened with a mesh screen and narrow plastic tubes.

2.2 Analysis Procedure

Flame temperature, concentrations of five stable chemical species, and fluorescence intensity of OH radical were measured and analyzed. Flame temperature was measured with a R-type (Pt-Pt13%Ph) thermocouple. The thermocouple was fixed on a xyz-stage. An absolute position was determined by using a reading-microscope, and displacement was measured by the micrometer of xyz-stage. The sensing part of thermocouple was a diameter of $25\mu\text{m}$, and it was coated with SiO_2 to prevent catalytic reactions. Flame gases were sampled by a quartz microprobe and analyzed with a gas chromatograph (SHIMADZU, GC-14B). This was equipped with a 3m SINCARBON-ST column. The microprobe was an outer diameter of 1.2mm and an inner diameter of 0.15mm. The sample was analyzed after dehumidification by silica gel. Concerning five stable species; O_2 , CO , CH_4 , CO_2 , and C_2H_6 , a proportional relation between peak area and mole fraction was obtained by an absolute calibration method. Fluorescence intensity of OH radical was measured by a PLIF method. Laser radiation was produced with a pulsed Nd:YAG laser (Spectra Physics, PIV400) and a dye laser (Sirah, PRSC-D-24). Q1(7) line of $\text{A}^2\Sigma^+ \leftarrow \text{X}^2\Pi(1,0)$ was selected; wavelength of the line was 283.2nm. The fluorescence intensity was monitored via an ICCD camera (Andor Technology, PH73425F-03). A lens for UV region (Nikon, PK-11A) and a bandpass filter (Asahi-Bunko, MY0310) were attached to the camera.

2.3 Numerical Procedure

A two-dimensional numerical calculation by using Konnov05 [5] mechanism was performed in a corresponding experimental condition. The calculation code was developed by Nishioka [6]. It used CHEMKIN subroutine [7, 8] to calculate thermochemical constants, reaction rates, and transport constants.

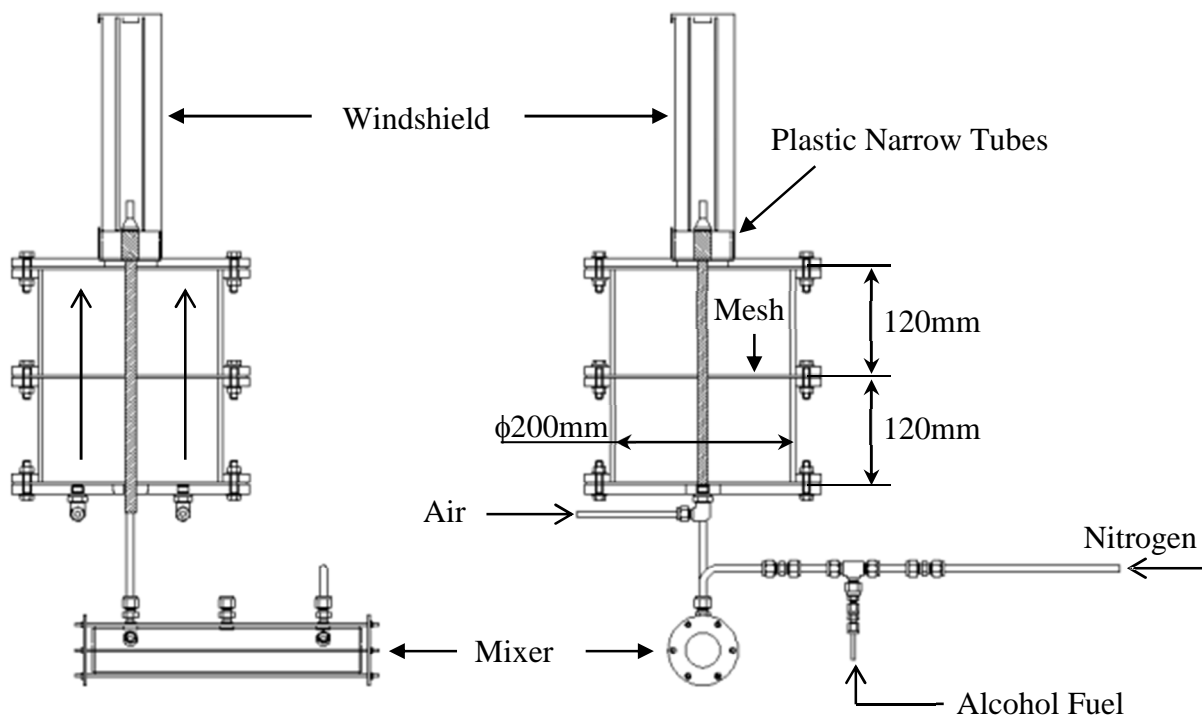


Figure 1. Schematic of the Vaporization System and the Burner (heaters are not drawn)

3 RESULTS

3.1 Ethanol Diffusion Flame

The experiment and calculation was conducted for 30vol% ethanol - 70vol% nitrogen diffusion flame. The condition is shown in Table 1. The volumetric flow rate of ethanol vapor was calculated with the following equation of state;

$$V_{e,g} = \frac{\rho_{e,l}}{M/V_0} \cdot \frac{T_g}{T_0} V_{e,l}$$

where $V_{e,g}$ and $V_{e,l}$ are the volumetric flow rate of gas ethanol and liquid ethanol respectively. T_0 and T_g is the temperature of ethanol at STP and vapor state. $\rho_{e,l}$ is the density of ethanol, and M is the molecular weight. The flow velocity of ambient air was half that of fuel stream, and the flow rate of the air was determined to fulfill this speed condition. The ethanol flame was stable during experiments. Figure 2 shows the positions of the thermocouple. The height from the burner rim was 5.15mm, 9.72mm, and 14.94 mm. Flame temperature profiles are shown in Figure 3 as a function of distance from the nozzle center. The thermocouple was moved with 0.2mm intervals in a horizontal direction. The accuracy of the temperature was expected to be better than $\pm 10K$. This includes a calibration error, a compensation lead wire error, and a general error of R-type thermocouple. Figure 4 shows chemical species concentration profiles at 9.72mm height. The mole fraction of OH radical from the numerical calculation is shown in Figure 5, and the fluorescence intensity of the radical from the experimental results is shown in Figure 6. The experimental result is the relative fluorescence intensity which was normalized by the maximum intensity.

The variation of the calculated temperature profile agreed with the experimental result. However, the calculated maximum temperature and the position where indicates the temperature didn't agree with the experimental result. The difference of these maximum temperatures increased as the measuring/calculating point was higher. Figure 6 shows that the position where indicates maximum intensity was almost same. In contrast, the numerical result, Figure 5, shows that the mole fraction of OH radical decreased as the calculating position was lower. Moreover, the position where indicates the peak of mole fraction moved to center of the burner as that. Accordingly, the calculated result by using Konnov05 mechanism did not reconstruct the ethanol flame height well.

Table 1: Condition of Ethanol Combustion

Total Fuel Gas Flow Rate [$10^{-5} \text{ m}^3/\text{s}$]	Nitrogen Flow Rate [$10^{-6} \text{ m}^3/\text{s}$]	Liquid Ethanol Flow Rate [$10^{-9} \text{ m}^3/\text{s}$]	Air Flow Rate [$10^{-4} \text{ m}^3/\text{s}$]
1.4	9.8	6.3	3.1

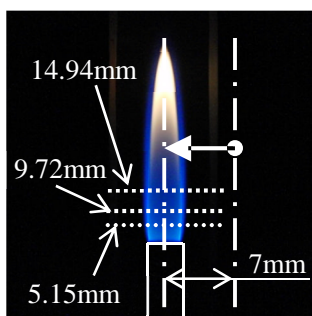


Figure 2. Positions of Flame Temperature Measurement

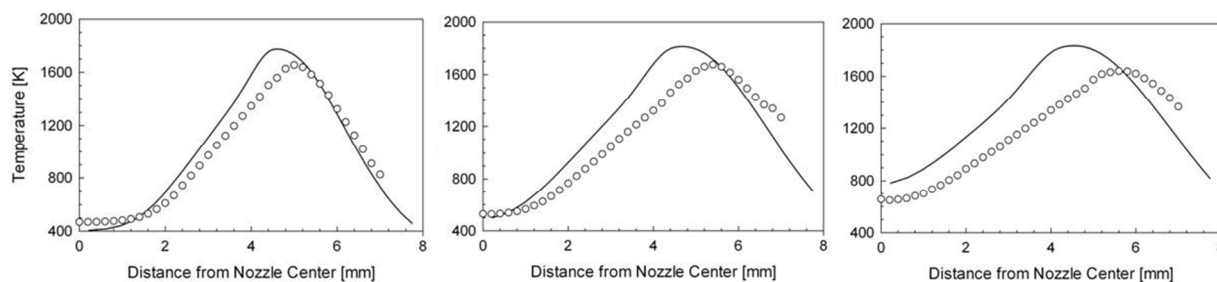


Figure 3. Temperature Profiles of Ethanol Flame.
 Left: height=5.15mm. Center: height=9.72mm. Right: height=14.94mm.
 The mark and the line show the results of experiment and calculation respectively.

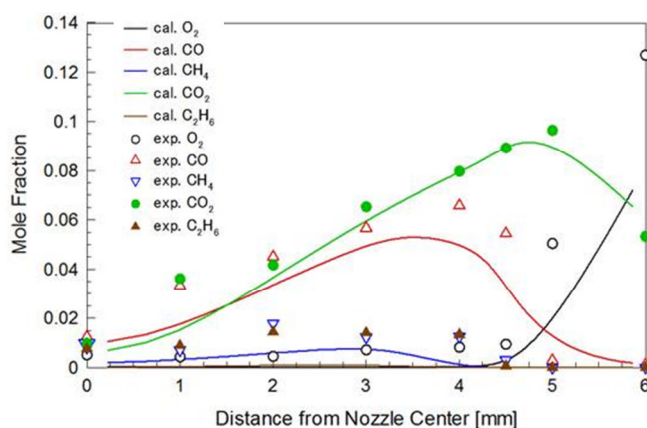


Figure 4. Chemical Species Concentration Profiles at 9.72mm Height

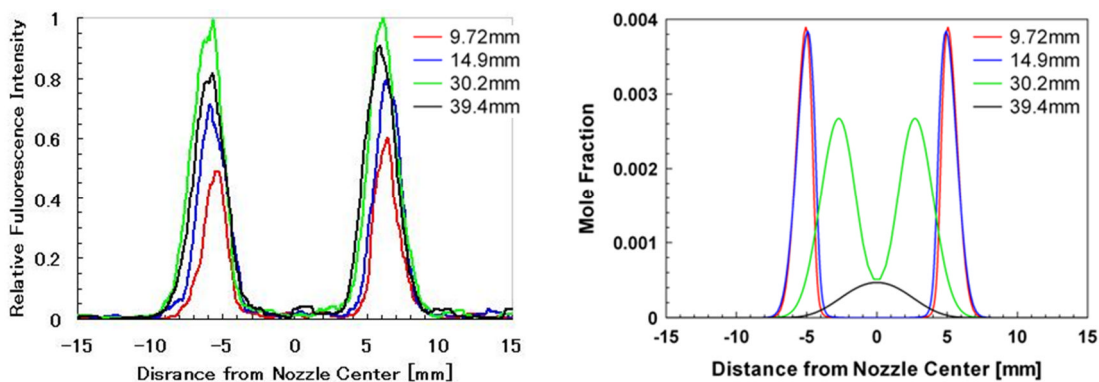


Figure 5. Distributions of OH radical.
 Left: Experiment Result, Right: Calculated Result

3.2 Methanol and Biomethanol Diffusion Flame

The experiment was conducted for 50vol% methanol - 50vol% nitrogen diffusion flame, and for 50vol% biomethanol diffusion flame. The condition is shown in Table 2. That of biomethanol is same. Figure 7 shows the positions of the thermocouple. Flame temperature profiles are shown in Figure 8 as a function of distance from the nozzle center. The height from the burner rim was 9.7mm.

Table 2: Condition of Methanol Combustion

Total Fuel Gas Flow Rate [$10^{-5} \text{ m}^3/\text{s}$]	Nitrogen Flow Rate [$10^{-6} \text{ m}^3/\text{s}$]	Liquid Methanol Flow Rate [$10^{-9} \text{ m}^3/\text{s}$]	Air Flow Rate [$10^{-4} \text{ m}^3/\text{s}$]
1.5	4.7	7.8	2.5

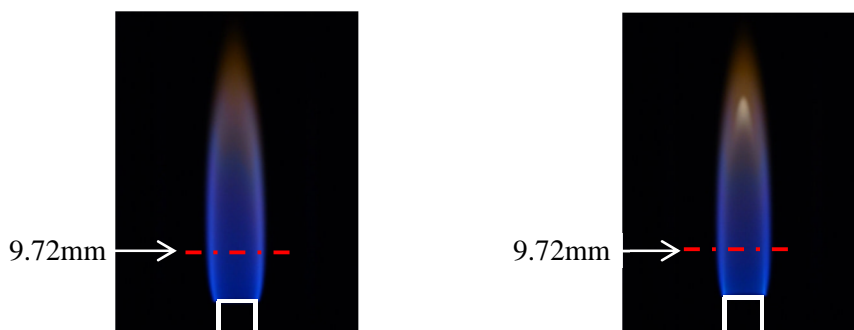


Figure 6. Positions of Flame Temperature Measurement
Left: Pure-Methanol Flame, Right: Biomethanol Flame

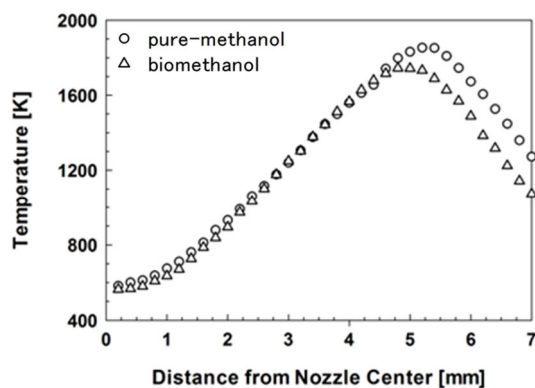


Figure 7. Temperature Profiles of Methanol and Biomethanol Flame

4 Conclusion

The new vapor system for liquid bio-alcohol fuel and the coflow burner were developed. Stable diffusion combustion with methanol, ethanol, and biomethanol was achieved. The two-dimensional numerical calculation using the detailed chemical kinetic mechanism was performed, and compared to the experimental results. The calculation in the condition corresponding to the experiment was

converged. However, there was difference between the experimental and calculated results at the higher measuring/calculating position. The calculated result using Konnov05 mechanism did not reconstruct ethanol flame height well. There are suitable mechanisms for methanol [9, 10] and ethanol [11] combustion, and these calculations are now executing.

References

- [1] Khizer Saeed, C.R. Stone, "Measurements of the laminar burning velocity for mixtures of methanol and air from a constant-volume vessel using multizone model," *Combustion and Flame*, 139, 2004, pp.152–166.
- [2] T.J. Held, F.L. Dryer, "An Experimental and computational study of methanol oxidation in the intermediate- and high-temperature regimes" *Proceedings of the Combustion Institute*, 25, 1994, pp.901-908
- [3] Shenghua Liu, Eddy R. Cuty Clemente, Tiegang Hu and Yanju Wei, "Study of spark ignition engine fueled with methanol/gasoline fuel blends," *Applied Thermal Engineering*, 27, 2007, pp.1904-1910
- [4] R. Seiser, S. Humer, K.Seshadri and E. Pucher, "Experimental investigation of methanol and ethanol flames in nonuniform flows," *Proceedings of the Combustion Institute*, 31, 2007, pp.1173-1180
- [5] A.A. Konnov, Detailed Reaction Mechanism for Small Hydrocarbons Combustion. Release 0.5, <http://homepages.vub.ac.be/~akonnov/>, 2000
- [6] M. Nishioka, T. Yamada, D.Kawamata, and Y. Kawaguchi, "Combustion Characteristics of Carbon Monoxide-Hydrogen-Nitrogen Coflow Diffusion Flame," *Journal of the Combustion Society of Japan*, 48, 143, 2006, pp.136-150
- [7] R.J. Kee, G. Dixon-Lewis, J. Warnatz, M.E. Coltrin and J. A.Miller, Sandia Report, "A Fortran computer package for the evaluation of gas-phase, multicomponent transport properties", SAND86-8246, 1986
- [8] R.J. Kee, F.M. Rupley and J.A. Miller, Sandia Report, SAND89-8009, "CHEMKIN-II: A Fortran Chemical Kinetics Package for the Analysis of Gas-Phase Chemical Kinetics", 1990
- [9] T. Held, F.Dryer, "A comprehensive mechanism for methanol oxidation," 30, 11, 1998, pp.805-830
- [10] Coda Zebetta, E., Hupa, M., "A detailed kinetic mechanism with methanol for simulating biomass combustion and N-pollutants," *Combustion and Flame*, 152, 2008, pp.14-27
- [11] Nick Marinov, "A detailed chemical kinetic model for high temperature ethanol oxidation," 31, 3, pp.183-220